Design of a Dual-Drive Mechanism for Precision Gantry

Heung-Keun Park, Sung-Soo Kim, Jin-Moo Park, Daehie Hong*
Department of Mechanical Engineering, Korea University, Seoul 136-701, Korea
Tae-Yeon Cho
Samsung Techwin Co., LTD, 145-3, Sangdaewon 1-Dong, Sungnam-City, Kyungki-Do, Korea

Gantry mechanisms have been widely used for precision manufacturing and material handling in electronics, nuclear, and automotive industries. Dual-drive servo mechanism is a way to increase control bandwidth, in which two primary axes aligned in parallel are synchronously driven by identical servo motors. With this mechanism, a flexible coupling (compliance mechanism) is often introduced in order to avoid the damage by the servo mismatch between the primary drives located at each side of gantry. This paper describes the design guidelines of the dual-drive servo mechanism with focus on its dynamic characteristics and control ramifications. That is, the effect on the system bandwidth which is critical on the system performance, the errors and torques exerted on guide ways in case of servo mismatch, the vibration characteristics concerned with dynamic error and settling time, and the driving force required at each axis for control are thoroughly investigated.

Key Words : Dual-drive Servo, Gantry, Flexible Coupling, Surface Mount Device, Chip mounter

1. Introduction

Dual-drive mechanism is used for increasing dynamic stiffness in some applications, such as transportation system of thin plate, overhead gantry crane, and electronic part assembly machines. Among these, the chip mounter, a circuit board assembly machine that places SMD (Surface Mount Device) electronic components on a printed circuit board, is under high demand for more fast and precise motion control. The objective of the dual-drive mechanism in the chip mounter is to transfer the head from one position to another as fast as possible, such that the settling time for the head location be minimized.

A simplified sketch of a typical gantry system with dual-drive mechanism is illustrated in Fig. 1.

* Corresponding Author,
  E-mail : dhhong@korea.ac.kr
  TEL : +82-2-3290-3369; **FAX** : +82-2-926-9290
  Department of Mechanical Engineering, Korea University, Seoul 136-701, Korea. (Manuscript **Received** May 7, 2002; **Revised** October 11, 2002)

Two stationary rails (Y₁, Y₂) aligned in parallel guide the motion of moving beam (X-axis) and this moving beam serves as the guide way for the moving head. Normally, one end of the X-axis is driven by a lead (or ball) screw installed on the Y-axis and the other end of the X-axis passively moves along the opposite Y-axis. The driving force is often transferred to the opposite Y-axis through appropriate mechanisms but there always exists a dead-band between the positions of the
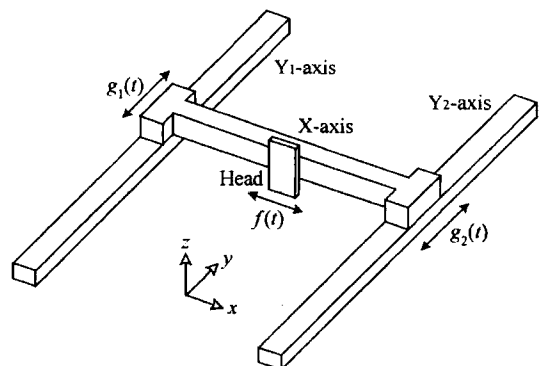

Fig. 1   Schematic of a dual-drive gantry mechanism

primary and the secondary Y-axes due to the backlash of these mechanical elements. This type of gantry mechanism is referred to as a 'single drive' mechanism in this paper.

Figure 2(a) shows the fundamental mode shape of the single drive gantry, which is equivalent to a cantilever beam. The fundamental frequency for a cantilever beam is very low and the system bandwidth is dictated by this mode. One of natural way to increase the bandwidth is shown in Fig. 2(b), where both ends are fixed to the Y-axes that are synchronously driven by identical actuators. In this way, the stiffness of the gantry system greatly increased, so that the control performance can be improved.

However, in case of an abnormal operation or in case that there exists twisting moments due to servo mismatch between the Y-axes, hazardous failure can occur at the major components. In addition, the friction force exerted on the linear motion guides due to the twisting moments can cause unwanted noise and severe wear. In order to prevent these problems, compliance mechanisms should be introduced, which can passively absorbs the adequate amount of twisting moment. That is, both ends of the X-axis are pin-jointed with torsional springs as shown in Fig. 2(c). However, adopting the compliance mechanism also causes the drawbacks such as curtailment of the system bandwidth and the amplification of the position error and settling time due to the loss of the stiffness at the boundary. Therefore, the effect of the compliance mechanism on the overall dynamic response and control should be carefully examined.
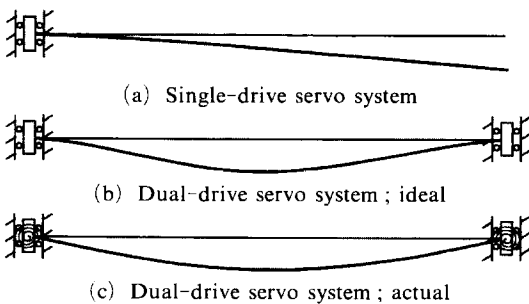
Up to now, some researchers have focused on synchronizing control algorithms between two servo drives (Kim et al., 2000 ; Lee, 1997 ; Shahruz and Pradeep, 1994) or establishing the equation of motion (Yoshikawa et al., 1993). The joint characteristics and compliance in robot manipulators have been also studied (Choi, 1996). However, few have considered the effect of this indispensable structural component on the system performance. This paper presents the reason why the compliance mechanism is needed for the dual drive servo mechanism, and then studied the effect of the compliance mechanism on the overall systems with respect to the categories that major concern. That is, the effect on the system bandwidth, the servo mismatch, the dynamic characteristic, and the driving force difference will be carefully investigated. The design procedures are illustrated with a case study. Through proper component designs, the performance of the overall system can be improved.

2. Design of Compliance Mechanism

Figure 3 shows the general factors that should be considered in compliance mechanism design. The design of compliance mechanism is a very complex task. The major design restrictions are on friction and wear of linear motion guide, control ability and margin for protection, safety of main parts, and system bandwidth.

At first, the joint stiffness can be determined by the endurable torque and allowable rotation. The torque at the joint should not be so high to
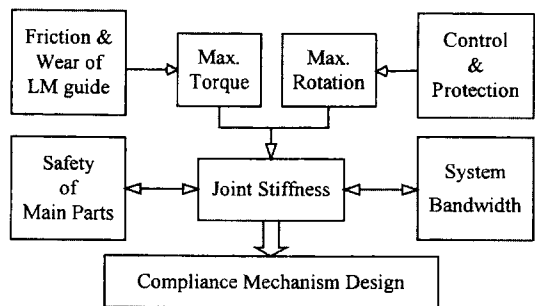
(a) Single-drive servo system

(b) Dual-drive servo system ; ideal

(c) Dual-drive servo system ; actual

Fig. 2 Fundamental mode shapes of three different servo configurations

Fig. 3 General factors in compliance mechanism design

prevent excessive wear in sliding parts. Friction force is generally known to be proportional to the contact force. Furthermore, the friction can induce unwanted noise. This reduces the life and precision of equipment. The allowable rotation is dictated by the maximum servo mismatch between two Y-axes, which accounts for disturbance bounds. Therefore, as the performance and robustness of the synchronous control are improved, the joint can be stiffened without the enlargement of the torque exerted on the linear guides.

However, the joint should be softer than any other part for safety. The main parts such as X and Y-axes, ball screws, linear motion guides should be protected from the permanent deformation or vibration induced fatigue due to control malfunction. The system bandwidth affects the control performance, which is usually treated as the most important design factor directly. It is also dependent on the joint stiffness.

Although there should be more to be considered, this paper studied the mechanical behavior of the overall dual-drive system with respect to the design categories mentioned above. That is, the effect on the system bandwidth which is critical on the system performance, the error and torque in case of servo mismatch, the dynamic characteristic concerned with dynamic error and settling time, and the driving force required to assist control.

3. System Bandwidth

The system bandwidth of a mechanical system is usually dictated by the fundamental natural frequency. This section describes the influence of the joint stiffness on the modal frequencies of the system. The fundamental frequency of the dual-drive servo with rigid joints is 6 times bigger than that of single-drive servo system. However, adopting the compliance mechanism causes the drawback to decrease the system bandwidth. The modal frequency of the beam with two torsional springs at the ends are given by the following empirical equation (Harris, 1988).

$$f_n = f_0 \left(\frac{2}{2n+1} \right)^2 \left[n + \frac{1}{2} \left(\frac{6\beta}{5+6\beta} \right) \right]^2 \qquad (1)$$
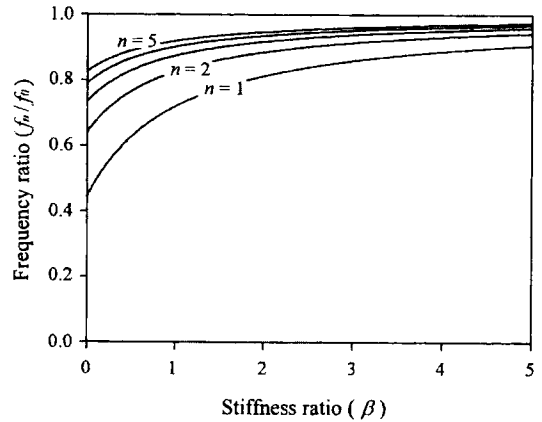

Fig. 4   Frequency ratio with respect to the joint stiffness ratio

where f_0 is the fundamental frequency of the beam with clamped ends, n is the mode number, and $\beta = k_{c\theta} l/6EI$ is the stiffness ratio of the joint and the beam. Also, $K_{c\theta}$ is the tortional stiffness of the joint and l, E and I are the length, elastic modulus, and area moment of inertia of the beam, respectively. Figure 4 shows the frequency ratio with respect to the stiffness ratio. The frequency ratio rapidly increases at low stiffness ratio and approaches to 1 as the stiffness ratio becomes higher. That is, the advantage obtained by increasing the joint stiffness is not so big, once it reaches a certain range. For example, the bandwidth will be down over 55% for the system with springs having negligible stiffness $(n=1, \beta=0)$. However, the shortening of the bandwidth can be reduced up to 20% with slightly higher stiffness $(n=1, \beta=2)$. Consequently, the plots in Fig. 4 give how the joint stiffness limits the system bandwidth, which can be utilized for the design and selection of the joint stiffness.

4. Head Position Error

The precise positioning capability is one of the most important factors in the fast dual-drive mechanism. The head position error of the gantry system consists of the error induced by the inertia loads due to the head and beam mass and the error induced by the servo mismatch, i.e., the synchronous error.

The deformation of the moving beam caused only by the inertia loads of the beam itself and the moving head can be determined by solving a quasi-static problem with uniformly distributed force and a concentrated force at the head location as

$$
\begin{aligned}
\delta_m&(f(t), t)\\
&=-\frac{w_a(t)\,l^4}{24EI}\left(\frac{f(t)}{l}\right)\left(1-\frac{f(t)}{l}\right)\left\{\frac{1}{1+3\beta}+\frac{f(t)}{l}\left(1-\frac{f(t)}{l}\right)\right\}\\
&\quad-\frac{2P_a(t)\,l^3}{6EI}\left(\frac{f(t)}{l}\right)^2\left(1-\frac{f(t)}{l}\right)^2\left[1-\frac{\beta}{1+\beta}\left\{\frac{5+6\beta}{2+6\beta}-\frac{f(t)}{l}\left(1-\frac{f(t)}{l}\right)\right\}\right]
\end{aligned}
\tag{2}
$$

where w_a and $P_a(t)$ are the y-directional inertia forces of the unit length of the beam and the head, respectively, and $f(t)$ is the position of the head along the X-axis.

The deformation due to the synchronous error can be represented by the displacement influence functions which describe the relative displacement at the head position due to a unit displacement at support restraints (Timoshenko et al., 1974). For the beam model with compliant supports at both ends, the displacement influence functions are described as

$$
\delta_1(f(t))=\frac{\beta}{1+\beta}\left\{2\left(\frac{f(t)}{l}\right)^2-3\left(\frac{f(t)}{l}\right)-\frac{1}{\beta}\right\}\left(\frac{f(t)}{l}\right)+1
\tag{3}
$$

$$
\delta_2(f(t))=-\frac{\beta}{1+\beta}\left\{2\left(\frac{f(t)}{l}\right)^2-3\left(\frac{f(t)}{l}\right)-\frac{1}{\beta}\right\}\left(\frac{f(t)}{l}\right)
\tag{4}
$$

where the subscripts 1 and 2 indicate the boundaries that undergo the unit displacement. Figure 5 shows the plots of the influence functions with a corresponding unit displacement. The resulting displacement is obtained by multiplying these influence functions with the displacements at each joint. The head position error is then produced by superposing the errors due to the inertia loads and the synchronous error, that is,

$$
\begin{aligned}
e_F(f(t), t)&=\delta_1(f(t))\,e_1(t)\\
&\quad+\delta_2(f(t))\,e_2(t)+\delta_m(f(t), t)
\end{aligned}
\tag{5}
$$

where $e_1(t)$ and $e_2(t)$ represent the tracking errors at each ends of the X-axis. Then, the actual head location in y-direction is the sum of this error and the commanded position,

$$
H(f(t), t)=g(t)+e_F(f(t), t)
\tag{6}
$$

where $g(t)$ is the specified commanded position of the head.

The rotational error at rest is caused only by the synchronous error and can be obtained by differentiating the first two terms in right hand side of Eq. (5) with respect to $f(t)$. Since it is independent to the absolute displacement of the boundaries, only the relative displacement error of the two servos contributes to the rotational error. Figure 6 shows the rotation error due to the unit displacement error between two drive axes. It can be seen that the error induced by the servo mismatch is somewhat critical in the sense of rotational error compared to the position error, because of the nonlinear characteristic of the position error. This can be an important factor especially in the application of chip mounter, because the rotational error may cause problems in chip alignment especially when locating big-sized chips.
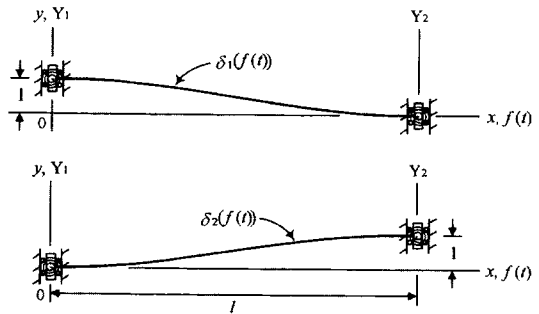

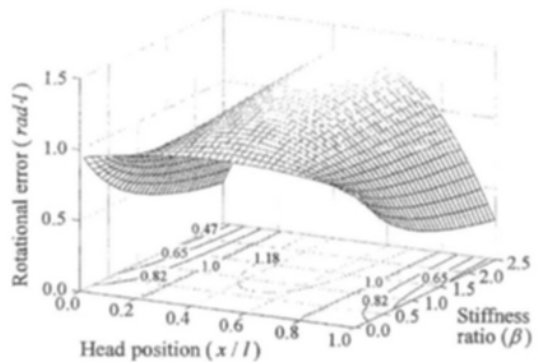**Fig. 5** Displacement influence functions

Fig. 6 Rotational error due to unit servo mismatch with respect to the joint stiffness and head position

5. Driving Forces

The forces acting on the carrier including the driving forces are depicted in Fig. 7. The major external forces acting on the carrier are induced by the gravity, inertia, and servo-mismatch. The forces and moments from the X-axis are transferred to the point A. The subscripts g and a are used to distinguish load types, which stands for gravity and acceleration, respectively. The x-directional moment M_t is due to the offset of the head mass center with respect to the shear center of the X-axis. The carrier is driven by ball screw at the point B with driving force F_{By} and moves along the linear motion guide (LM guide) attached at the supporting points LM_1, LM_2. Each point has two reaction force components in x and z-directions. The y-directional moment at the LM guide is M_{LM} and R_{LMF} is the friction force due to these reaction forces along the LM guide. The LM guide is assumed to withstand the loads and moments in all directions resulting from the external forces.

The reaction forces and moments on a beam with clamped ends are represented as the following equations (Pilkey, 1994). That is, the moments in y-direction and the forces in z-direction due to gravity are described as

$$M_{g1} = \frac{w_g l^2}{12} + P_g \frac{f(t)}{l}\left(1 - \frac{f(t)}{l}\right)^2 \qquad (7)$$

$$M_{g2} = \frac{w_g l^2}{12} + P_g\left(\frac{f(t)}{l}\right)^2\left(1 - \frac{f(t)}{l}\right) \qquad (8)$$
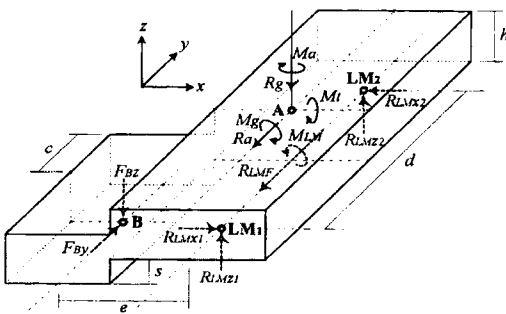
Ball screw   LM guide

Fig. 7   Forces and moments exerted on the carrier

$$R_{g1} = \frac{w_g l}{2} + P_g\left(1 - \frac{f(t)}{l}\right)^2\left(1 + 2\frac{f(t)}{l}\right) \quad (9)$$

$$R_{g2} = \frac{w_g l}{2} + P_g\left(\frac{f(t)}{l}\right)^2\left(3 - 2\frac{f(t)}{l}\right) \qquad (10)$$

where w_g and P_g are the weight per unit length of the beam and the weight of the moving head, respectively, $f(t)$ is the position of the head along the X-axis, and the subscripts 1 and 2 indicate each joints.

On the contrast, including the stiffness of compliance mechanism at both ends, the moments and forces can be represented by the following equations. These equations are describing the moments in z-direction and forces in y-direction due to the inertia forces by the moving parts.

$$M_{a1} = \frac{\beta}{1+3\beta}\frac{w_a l^2}{4}$$
$$+ \frac{\beta}{(1+\beta)(1+3\beta)}\left\{1 + (1+3\beta)\left(1 - \frac{f(t)}{l}\right)\right\}\left(1 - \frac{f(t)}{l}\right)f(t)P_a \qquad (11)$$

$$M_{a2} = \frac{\beta}{1+3\beta}\frac{w_a l^2}{4}$$
$$+ \frac{\beta}{(1+\beta)(1+3\beta)}\left\{1 + (1+3\beta)\frac{f(t)}{l}\right\}\left(1 - \frac{f(t)}{l}\right)f(t)P_a \qquad (12)$$

$$R_{a1} = \frac{w_a l}{2} + \left\{1 - \frac{\beta}{(1+\beta)}\left(\frac{2f(t)}{l} - 1\right)\frac{f(t)}{l}\right\}\left(1 - \frac{f(t)}{l}\right)P_a \quad (13)$$

$$R_{a2} = \frac{w_a l}{2} + \left\{1 + \frac{\beta}{(1+\beta)}\left(\frac{2f(t)}{l} - 1\right)\left(1 - \frac{f(t)}{l}\right)\right\}\frac{f(t)}{l}P_a \quad (14)$$

where w_a and P_a are the y-directional inertia forces of the unit length of the beam and the head, respectively. Figure 8 shows the moment at the joint 1 and the moment difference between two joints under constant acceleration with respect to the joint stiffness and head position. Since the moment due to the beam itself is independent of the head position, it is not included in the figure. As can be seen from the figure, relatively large compliance (small β) should be used to reduce the moment. For example, the moment is reduced only in half by reducing the stiffness up to $\beta = 0.5$. This means the loss of the bandwidth is almost 40% as shown in Fig. 4. On the other hand, the variation of the values around $\beta = 2.0$ is small enough to ignore the moment change caused by adjusting the joint stiffness.
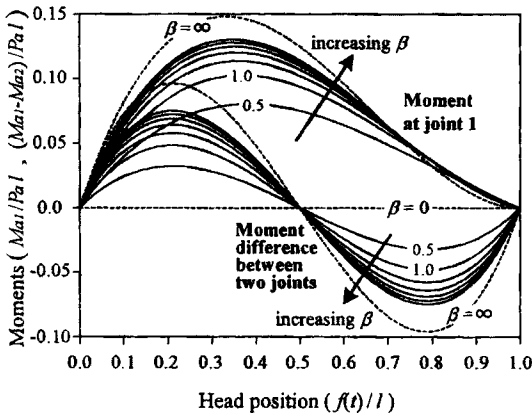
Fig. 8 Moment at the joint 1 and moment difference between two joints with respect to the joint stiffness and head position

The x-directional moment due to the offset of the head mass center with respect to the shear center of the X-axis is due to the gravitational force P_g and the inertial forces P_a of the head, which is

$$M_t = \varepsilon_y P_g + \varepsilon_z P_a \qquad (15)$$

where ε_y and ε_z are the offset distances in y and z-directions, respectively.

The moment in z-direction due to the servo mismatch between two joints are described by the following equation,

$$M_{\delta y} = EI \frac{\beta}{1+\beta} \frac{6\delta_y}{l^2} \qquad (16)$$

where δ_y is the magnitude of the mismatch between two joints, which is defined as

$$\delta_y = g_2(t) - g_1(t) \qquad (17)$$

Thus, the total moments acting on the joints in z-direction are the sums of the moments in Eqs. $(11) \sim (12)$ and the moment in Eq. (16).

Applying the equilibrium conditions to the carrier model, the reaction forces on the LM-guide can be determined. Further, the friction force due to these reaction forces will be

$$R_{LMF} = \mu \left(\sum_{i=1}^{2} |R_{LMxi}| + \sum_{j=1}^{2} |R_{LMzj}| + F_{LM} \right) \qquad (18)$$

where μ is the friction coefficient of the LM-guide and F_{LM} is the equivalent friction force due to the M_{LM} with the relation,

$$F_{LM} = K_c \cdot M_{LM} \qquad (4)$$

where K_c is the corresponding conversion factor. The driving force F_{By} is then,

$$F_{By} = R_a + R_{LMF} \qquad (20)$$

where R_a is the force in y-direction due to the acceleration of the moving parts in Eqs. $(13) \sim (14)$.

The reaction force in z-direction has positive or negative values according to the driving conditions and geometry. Thus, the driving force in each case is as follow.

i) $R_{LMZ1} > 0$, $R_{LMZ2} > 0$

$$F_{By} = \frac{d}{d-2e\mu} \left\{ R_a + \mu \left(R_g + \frac{2M_a}{d} + F_{LM} + \frac{M_g - M_{LM}}{e} \right) \right\} \qquad (21)$$

ii) $R_{LMZ1} < 0$, $R_{LMZ2} > 0$

$$F_{By} = \frac{d}{d-2(e-s)\mu} \left\{ R_a + \mu \left[\frac{2}{d} \left(M_a + M_t - hR_a \right) - \frac{c}{e} (M_g - M_{LM}) \right) + F_{LM} \right] \right\} \qquad (22)$$

where M_{LM} is the y-directional moment which is resisted by the LM-guide. If the LM-guide has load ratings larger than the M_g, then the term $(M_g - M_{LM})$ in the above equations will be vanished. Therefore, the LM-guide should be carefully selected. Otherwise, the term mentioned above exists and results in the transverse reaction force acting on the ball-screw, shown as F_{BZ} in Fig. 7. Then, the deformation of the ball-screw can make another problem like a fluctuating motion.

Another interesting aspect in designing the dual-drive system is to avoid self-locking conditions. From Eqs. $(21) \sim (22)$, it can be seen that the self-locking will occur when the denominator of the equations reaches zero, i.e.,

$$(d - 2e\mu) \to 0, \quad (d - 2(e-s)\mu) \to 0 \qquad (23)$$

In this situation, infinite amount of the driving forces is needed to move the X-axis. In order to prevent this, the distance between two supporting points in the LM-guide should be big enough, or the distance between the ball screw and the LM-guide be short enough. Also, the smaller friction coefficient is preferred.

In general driving conditions, the driving forces are governed by Eq. (21) and the additional driv-
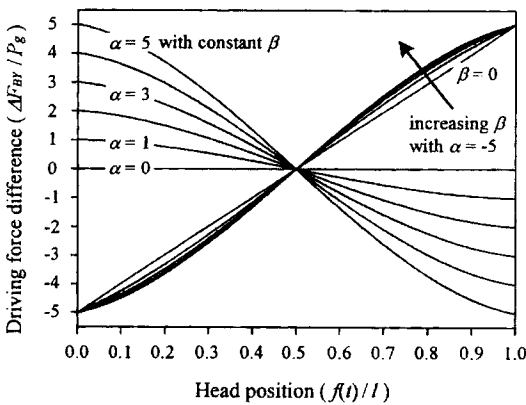
Fig. 9 Differences in driving forces between two axes with respect to the joint stiffness, moving acceleration, and head position

ing force needed in the axis 1 with reference to the axis 2 is then

$$\Delta F_{By} = \frac{d}{d-2e\mu}\left\{(a+\mu) + \left[\frac{2\alpha\beta}{1+\beta}\left(1+\mu\frac{l}{d}\right)\right.\right.$$
$$\left.\left. + \mu(2+K_c l)\right]\left(1-\frac{f(t)}{l}\right)\frac{f(t)}{l}\right\}\left(1-\frac{2f(t)}{l}\right)P_g \quad (24)$$

where α is the ratio of the moving acceleration a to the gravitational constant g. The graphical representations are depicted in Fig. 9. The driving force differences under constant acceleration varies in relatively small amount as the joint stiffness varies but the acceleration acts as a key factor.

6. Design Example

For further understanding, a simple design example is included in this section. The design procedure of a dual drive servo system with compliance mechanism is depicted in Fig. 10. The required task is to transport the head of 20 kg with maximum acceleration of 40 m/s². The associated system requirements are the system bandwidth, the static deflection, the head position error, and the allowable torque (these values for this example are shown in Fig. 10). It is assumed that the controller can restrict the synchronous error under 40 μm in normal condition and the actual positions of the two joints are always in this bound. To protect the system, the error be-
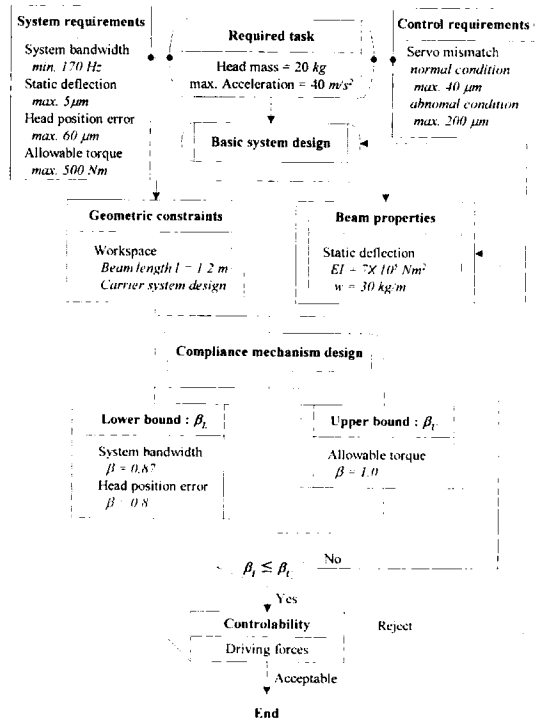

Fig. 10 Design procedure of dual drive mechanism

tween two joints is allowed up to 200 μm in abnormal condition.

The first step is to build the system to meet some of the basic requirements, which is independent of the compliance mechanism. In most design problems, the workspace is predetermined, so the beam length and carrier sub-system are almost fixed. Then, the basic beam-mass system can be built to meet the static deflection, the deflection of the beam-mass system under gravitation force. The reason for using static deflection as a basic step is that the beam-mass system with fixed ends gives near upper bound in the sense of dynamic and static properties.

Next step is to determine the stiffness ratio of the compliance mechanism. The required system bandwidth and head position error can be served as the decision guide to determine the lower bound of the allowable stiffness ratio. The basic system built through the first step has fundamental mode of 378 Hz without head and 242 Hz with head. From Eq. (1) or Fig. (4), the minimum stiffness ratio can be determined as 0.87 or bigger
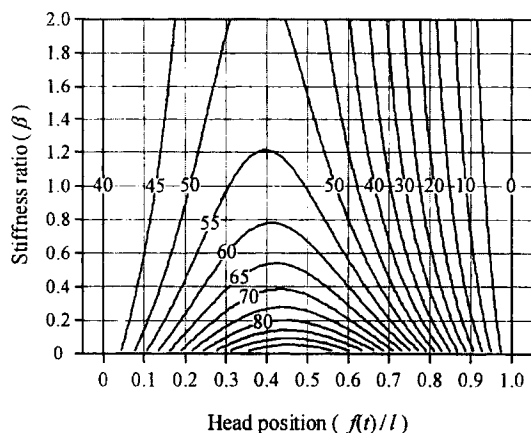
Fig. 11 Head position error with respect to the joint stiffness and head position (unit= μm, synchronous error=40 μm, acceleration= 40 m/s^2)

to meet the required system bandwidth, 170 Hz. The head position error during motion is depicted in Fig. 11 including the servo mismatch under normal condition. The maximum position error occurs when one end is delayed as 40 μm during motion of maximum acceleration. From Eq. (5) or Fig. 11, the stiffness ratio should be larger than about 0.8 to restrict the head position error under 60 μm. Therefore, lower limit of the stiffness ratio can be determined as 0.87 to satisfy both restrictions. The corresponding upper bound can be determined to meet the allowable torque. In this case, the servo mismatch error in abnormal condition is used to calculate the torque induced by mismatch. From Eqs. (11) and (16), to restrict the torque under 500 Nm, the stiffness ratio should be less than 1.0. As such, the stiffness ratio is within acceptable range. However, if the calculated value is out of the range, the procedures should be repeated, in which more stiff and lighter material for the beam must be selected.

Finally, the driving force difference presented in Eq. (24) should be checked. Since the driving force difference has little dependence on the compliance, as can be seen from Fig. 9, unless the driving force difference is too severe to accept, the design of the basic system would meet all the system design requirements.

7. Conclusion

This paper provides a general concept of dual-drive servo mechanism and gives its design guidelines with focus on the effect of system bandwidth, the error and torque in case of servo mismatch, and the driving force required at each axis to overcome friction forces. In general, it is concluded that the frequency bandwidth can be greatly increased by adopting the dual-drive mechanism but once the compliance mechanism is chosen, the curtailment of the frequency-band is inevitable. However, the shortening of the band can be reduced up to 20% with slightly controlling the stiffness. The error induced by the servo mismatch is obtained by introducing the displacement influence function. Finally, by modeling the driving part, the required driving forces of each axis are determined through quasi-static analysis. These equations give the information about the driving force required to prevent the mismatch between dual axes and geometric considerations to prevent self-locking. The driving force differences under constant acceleration varies relatively small amount as the joint stiffness varies but the acceleration acts as a key factor.

Acknowledgment

References

Choi, H. R., Chung, W. K. and Youm, Y., 1996, "A Method of Compliance Control of Redundant Manipulators," *KSME International Journal*, Vol. 10, No. 2, pp. 119~127.

Harris, C. M., 1988, *Shock and Vibration Handbook*, McGraw-Hill, New York.

Kim, B. K., Chung, W. K., and Suh, I. H., 2000, "Robust Synchronizing Motion Control of Twin-Servo System Based on Network Modeling," *Proc. 2000 IEEE Int. Conf. on Decision*

and Control, Sydney, Australia, pp. 1019~1024.

Lee, G. B., 1997, "A Receding Time Horizon Optimal Feedrate Control with Cross Coupled Structure for Multiaxial Systems," *KSME International Journal*, Vol. 11, No. 4, pp. 419~427.

Park, H. K., Kim, S. S., Park, J. M., Cho, T. Y. and Hong, D., 2001, "Dynamics of Dual-Drive Servo Mechanism," *Proc. 2001 IEEE Int. Symp. on Industrial Electronics*, Pusan, Korea, pp. 1996~2000.

Pilkey, W. D., 1994, *Formulas for Stress, Strain, and Structural Matrices*, John Wiley & Sons, New York.

Shahruz, S. M. and Pradeep, A. K., 1994, "High Precision Synchronizing Control System for Biaxial Positioning Tables," *Trans. ASME Journal of Dynamic Systems, Measurement and Control*, Vol. 116, pp. 158~163.

Timoshenko, S., Young, D. H. and Weaver JR, W., 1974, *Vibration Problems in Engineering*, John Wiley & Sons, New York.

Yoshikawa, T., Hosoda, K., Harada, K. and Ichikawa, M., 1993, "Trajectory Control of Cartesian Type Industrial Manipulators with Flexible Joints," *Proc. 1993 IEEE/RSJ Int. Conf. on Intelligent Robots and Systems*, Yokohama, Japan, pp. 14~21.